Anomalous Behavior in the Nucleation of Ice at Negative Pressures

Valentino Bianco,* P. Montero de Hijes, Cintia P. Lamas, Eduardo Sanz, and Carlos Vega†
Departamento de Quimica Fisica, Facultad de Quimica, Universidad Complutense de Madrid, Ciudad Universitaria, Madrid 28040, Spain

(Received 29 July 2020; revised 14 October 2020; accepted 8 December 2020; published 8 January 2021)

Ice nucleation is a phenomenon that, despite the relevant implications for life, atmospheric sciences, and technological applications, is far from being completely understood, especially under extreme thermodynamic conditions. In this work we present a computational investigation of the homogeneous ice nucleation at negative pressures. By means of the seeding technique we estimate the size of the ice critical nucleus N_c for the TIP4P/Ice water model. This is done along the isotherms 230, 240, and 250 K, from positive to negative pressures until reaching the liquid-gas kinetic stability limit (where cavitation cannot be avoided). We find that N_c is nonmonotonic upon depressurization, reaching a minimum at negative pressures in the doubly metastable region of water. According to classical nucleation theory we establish the nucleation rate J and the surface tension γ, revealing a retracing behavior of both when the liquid-gas kinetic stability limit is approached. We also predict a reentrant behavior of the homogeneous nucleation line. The reentrance of these properties is related to the reentrance of the coexistence line at negative pressure, revealing new anomalies of water. The results of this work suggest the possibility of having metastable samples of liquid water for long times at negative pressure provided that heterogeneous nucleation is suppressed.

DOI: 10.1103/PhysRevLett.126.015704

Ice formation is possibly the most important liquid-to-solid transition, being relevant in cryobiology, food storage, material science, and Earth science [1–8]. Homogeneous nucleation is the mechanism through which thermal fluctuations in a pure liquid below coexistence induce the formation of crystal nuclei that, when sufficiently large (critical size), trigger the crystallization.

At ambient pressure and a few kelvins below coexistence, the size of the critical nucleus N_c is huge and the probability of forming spontaneously in pure supercooled water is negligible [9,10]. Consequently, in nature, ice is formed essentially via heterogeneous nucleation [11].

Several investigations have addressed the behavior of supercooled liquid water at negative pressure [12–20], with little attention paid to ice nucleation [21,22]. Here, we fill this gap by exploring the homogeneous ice nucleation from positive to negative pressure P at constant temperature T.

By means of molecular dynamic simulations of the TIP4P/Ice water model [23]—probably the best atomistic model to study ice properties and with a well known phase diagram[23,24]—we reveal that the isothermal variation of N_c is nonmonotonic. For any isothermal path, a minimum is always observed at $P < 0$. This retracing behavior is linked to the reentrance of the coexistence line.

All the simulations have been performed using GROMACS [25], adopting (i) a time step of 2 fs; (ii) the Noose-Hoover thermostat with a relaxation time of 1 ps; (iii) the Parrinello-Rahman barostat with a relaxation time of 2 ps; (iv) the particle-mesh-Ewald algorithm of order 4, with Fourier spacing of 0.1 nm to solve the electrostatic interaction; (v) a cutoff of 0.9 nm both for the Lennard-Jones and Coulomb interactions; (vi) long range corrections to the Lennard-Jones interaction.

Given the polymorphism of ice, we investigate the most stable structure. According to Matsui *et al.* [26], Ih is clearly the most stable ice up to extreme negative pressures, where ice Ih and the recently discovered ice XVI [27] are close in terms of stability. Hence, first we determine the solid-liquid coexistence lines for ice Ih and ice XVI for the TIP4P/Ice model via direct coexistence simulations [see the Supplemental Material (SM) [28]]. The T-P loci of the coexistence lines are shown in Fig. 1(a). For $P > -3000$ bar the ice XVI coexistence line is lower than the Ih coexistence line, meaning that the Ih structure is more stable than the ice XVI for this pressure range. The triple point water-Ih-ice XVI is estimated at $P \sim -3000$ bar and $T \sim 278$ K, similar to what has been found for the TIP4P/2005 water model [29]. Therefore, we have conducted our investigation with ice Ih, although for $P < -3000$bar the nucleation of ice XVI could be relevant.

We then estimate the liquid-gas kinetic stability limit defined as the $T-P$ locus where 2000 liquid water molecules were stable for at least 100 ns. For any thermodynamic state in this work it is possible to reach a metastable equilibrium, as the relaxation time is smaller than 40 ns [Fig. 1(b)]. As can be seen, before this stability limit is reached, there is a reentrance of the coexistence line with a turning point $dT/dP = 0$ at $P \sim -2000$ bar and $T \sim 280$ K.

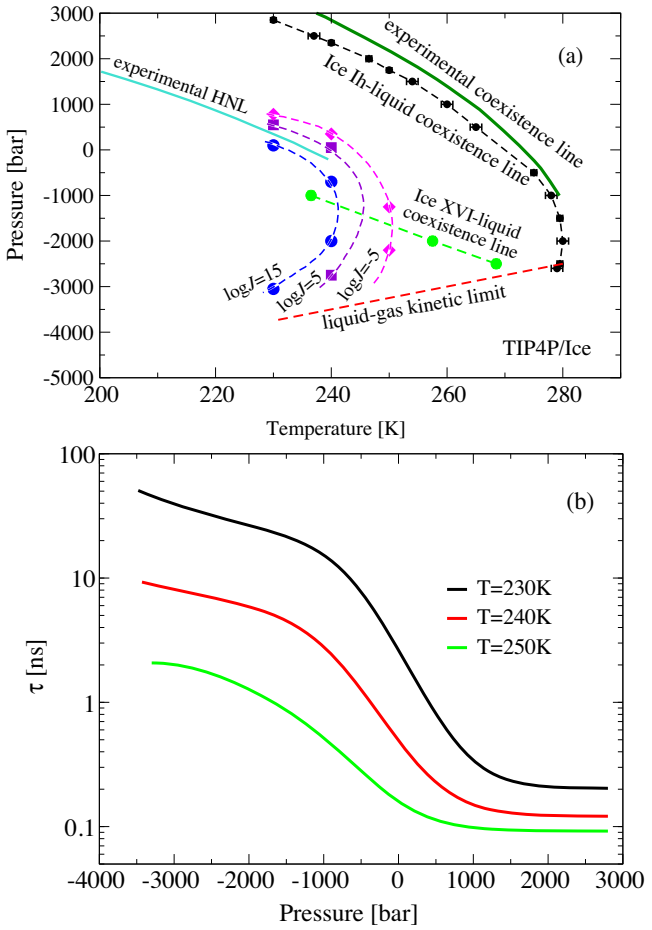

FIG. 1. (a) Phase diagram in the T–P plane of the TIP4P/Ice water model showing (i) the ice Ih-liquid coexistence line (black points); (ii) the liquid-gas kinetic limit (red dashed line); (iii) the isolines with constant logarithm of the nucleation rate: $\log_{10} J/(\mathrm{m}^{-3}\,\mathrm{s}^{-1}) = 15, 5, -5$ [see Fig. 4(b)]. (iv) the fitting of experimental homogeneous nucleation line (HNL) [22] and ice Ih-liquid coexistence proposed by Marcolli [21]; (v) the ice XVI-liquid coexistence curve (green points). The HNL (where the formation of ice can not be avoided) from experiments corresponds approximately to an isoline $\log_{10} J/(\mathrm{m}^{-3}\,\mathrm{s}^{-1}) = 15$ [9]. (b) Relaxation time $\tau \equiv (0.31\,\mathrm{nm})^2/(6D)$ to diffuse the diameter of a water molecule as a function of P.

In 1982, Speedy conjectured a reentering behavior of the liquid-gas spinodal [30]. This has been recently demonstrated to be the case for colloidal systems [31] but ruled out for water [32] as further seen in this work. Nevertheless, Henderson and Speedy later conjectured a reentrance in the coexistence line [15] (also suggested by Bridgman [33]). Speedy's estimation of the turning point of the coexistence line occurring at $P \sim -1750$ bar and $T \sim 283$ K [15] is surprisingly close to our numerical finding.

Although experimentally inaccessible for large (in absolute value) negative pressures, the possible reentrance of the solid-liquid coexistence line affects the kinetic and thermodynamic properties of the accessible metastable region of the supercooled water's phase diagram at negative pressure. This phenomenon resembles what has been largely discussed in the last decades about the origin of water's anomalies [7,19,34–44]. There, the possible presence of a second liquid-liquid critical point in a low T-high P region of the phase diagram (confirmed recently for the TIP4P/Ice model [24] although experimentally prohibitive) would determine the increase of the fluctuations (and related thermodynamic response functions) in the accessible metastable region of the phase diagram.

To evaluate N_c we follow the *seeding* computational approach, introduced by Bai and Li [45], and widely adopted in nucleation studies [11,46–60] (see SM for details). This scheme consists in introducing a spherical crystal seed of a given size into a bulk of supercooled liquid and let it evolve at constant T and P. Seeds whose size is larger than $N_c(T,P)$ grow spanning the entire system, while those below $N_c(T,P)$ melt. When the size is critical, the crystal seed can grow or melt with equal probability. Hence, by comparing the time evolution of the size of the crystal seeds at certain T and P, it is possible to establish N_c (within a certain resolution). One can either study seeds differing in size at fixed state point $T-P$ [Figs. 2(a)–2(c)] or a given seed at different T-P [Fig. 2(d)].

We investigate the $T = (230, 240, 250)$ K isotherms with $N \sim 46\,000$ water molecules. For any T we explore $P \in [-3500\!:\!2400]$ bar, i.e., from the liquid-gas kinetic

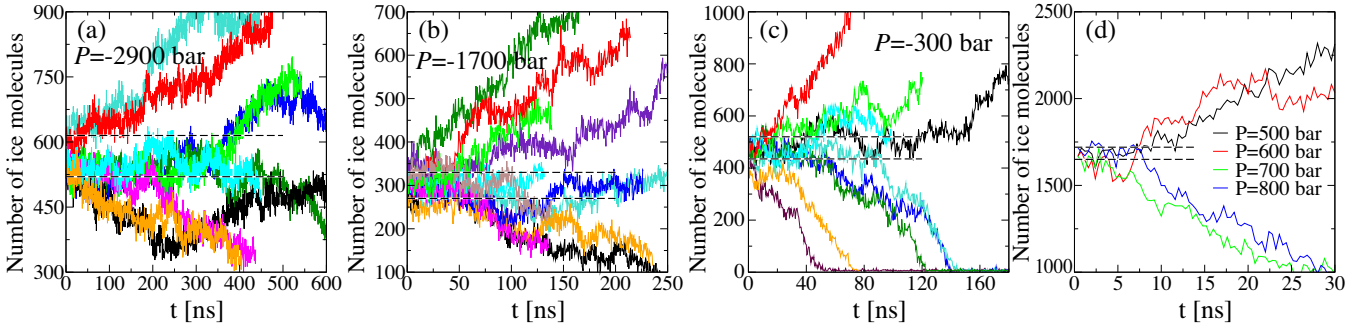

FIG. 2. Time evolution of the ice seed along the isotherm $T = 240$ K at (a) $P = -2900$ bar; (b) $P = -1700$ bar; (c) $P = -300$ bar; (d) different positive pressures. Dashed lines mark the boundaries of the estimated critical size N_c (established as the difference between the size of the largest seed melting and the smallest seed growing). In (a)–(c) P was constant and we changed the size of the initial ice cluster. In (d), the initial size of the cluster was identical but it was studied at different P. From the results of (d) one estimates that the cluster is critical at $P \sim 650$ bar.

stability limit at negative pressures up to the melting point at positive pressures. The number of ice molecules is determined according to the Lechner-Dellago order parameter $\bar{q}_6$ [61], with cutoff distance of 3.5 Å. Molecules (within the cutoff distance) above the threshold $\bar{q}_{6,t}$ are labeled as ice, whereas those with smaller values are labeled as liquid. The value of $\bar{q}_{6,t}$ which depends on P and T is determined according to the mislabeling criterion [47] (see the SM for details). In Fig. 2 we show the time evolution of the number of ice particles in the crystal seed along the isotherm $T = 240$ K, with runs spanning in some cases up to the μs. On average any N_c has been identified by means of ~10 independent runs. All the estimated N_c along the three isotherms are presented in Fig. 3(c) and reported in the SM. As shown in Fig. 3(c), from positive pressures, N_c largely decreases upon decreasing P, reaching a quasiconstant value at negative P. By further decreasing P we find that N_c increases again. In all cases the minimum value of N_c is observed at $P < 0$. In particular, we find that the minimum value of N_c is ~150 for $T = 230$ K, ~310 for $T = 240$ K, and ~800 for $T = 250$ K. From $N_c(T, P)$ we can extract the P dependence of the surface tension $\gamma(T, P)$ following the classical nucleation theory (CNT). Indeed, according to CNT, γ can be expressed as [48]

$$\gamma(T,P) = \left[\frac{3\rho_{\mathrm{ice}}(T,P)^2|\Delta\mu(T,P)|^3 N_c(T,P)}{32\pi}\right]^{1/3}, \quad (1)$$

being $\rho_{\mathrm{ice}}(T, P)$ the ice density at (T, P), and $\Delta\mu(T, P) \equiv \mu_{\mathrm{liq}}(T, P) - \mu_{\mathrm{ice}}(T, P)$ the difference in chemical potential between water (μ_{liq}) and ice (μ_{ice}). As discussed in the SM (see Fig. 3 and Table II), $\Delta\mu$ can be computed by thermodynamic integration. In Fig. 3(a) we report $\Delta\mu$ along the isotherms of interest, showing a retracing behavior whose maximum value is always reached at $P < 0$. The maxima of $\Delta\mu$ are observed at $(T = 230\ \mathrm{K}, P \sim -1160\ \mathrm{bar})$, $(T = 240\ \mathrm{K}, P \sim -1405\ \mathrm{bar})$, and $(T = 250\ \mathrm{K}, P \sim -1605\ \mathrm{bar})$, roughly coinciding with the thermodynamic state points where $N_c(P)$ exhibits a minimum. The presence of the maximum of $\Delta\mu$ is due to the crossing of ice and liquid water densities along the corresponding isotherm as shown in Fig. 3(a) inset [see also Figs. 3(c)–3(e) of the SM]. From Eq. (1) we obtain γ which is shown in Fig. 4(a). As can be seen, γ decreases upon decreasing P, reaching a quasiconstant value at negative P, then increasing again at largely (in absolute value) negative P. We can extract the values of γ at $P = 1$ bar: $\gamma \sim 20\ \mathrm{mJ/m^2}$ for $T = 230$ K, $\gamma \sim 21\ \mathrm{mJ/m^2}$ for $T = 240$ K, and $\gamma \sim 24\ \mathrm{mJ/m^2}$ for $T = 250$ K. These values are in agreement with the fitting expression for $\gamma(T, P = 1\ \mathrm{bar})$ reported in Refs. [48,52] ($\gamma = 19.1$, 21.8, 24.5 $\mathrm{mJ/m^2}$, respectively).

Following Becker and Döring [62] we can express the nucleation rate $J(T, P)$ as

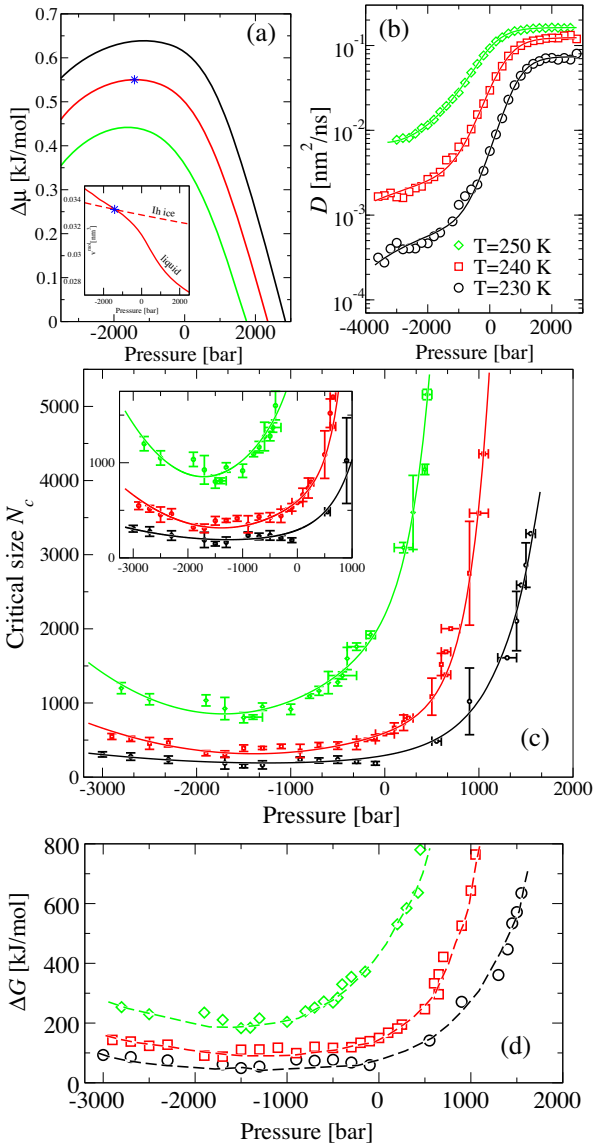

FIG. 3. Different observables as a function of P along the isotherms $T = 230$ K, $T = 240$ K, and $T = 250$ K [legend for all panels in (b)]: (a) Difference in chemical potential $\Delta\mu$. Volume per molecule of Ih ice and liquid water at $T = 240$ K in inset. Blue star indicators are at the same P. (b) Diffusion coefficient D. Lines are fitting curves reported in the SM. (c) Size of the ice critical nucleus N_c. Inset shows an enlargement of the region where the minima are observed. Lines are fitting functions given in the SM. (d) Gibbs free energy barrier ΔG (enlargement at the minima including error bars in SM). Dashed lines are guides for the eye.

$$J(T,P) = \rho_{\mathrm{liq}} f^+ Z \exp(-\Delta G_c/k_B T), \quad (2)$$

where ρ_{liq} is the density of the liquid phase, and $\Delta G_c = N_c|\Delta\mu(T, P)|/2$ is the free energy barrier associated with the formation of a critical cluster. Also, k_B is the Boltzmann constant and $Z \equiv \sqrt{|\Delta\mu|/(6\pi k_B T N_c)}$ is the Zeldovich factor which depends on the curvature of ΔG around the

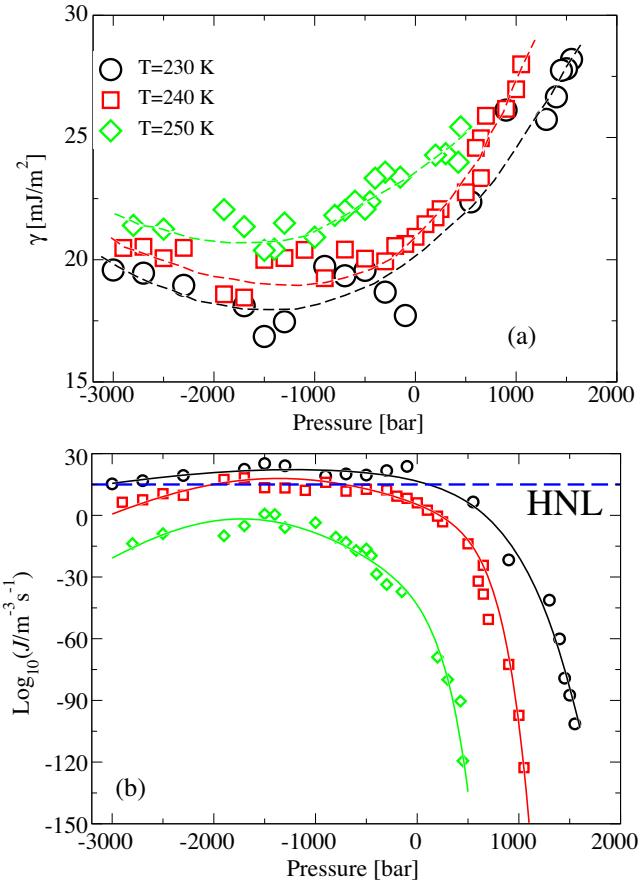

FIG. 4. Isothermal variations (at 230, 240, and 250 K) with P of (a) Surface tension γ. Dashed lines are guides for the eye. (b) The logarithm of J (enlarged at the maxima including error bars in SM). Same legend as (a). Dashed blue line marks the homogeneous nucleation line (HNL) given by $\log_{10} J/(\mathrm{m}^{-3}\,\mathrm{s}^{-1}) = 15$. Continuous lines are an analytical expression according to Eq. (2), using the fitting curves $\rho_{\mathrm{liq}}(T,P)$ shown in Fig. 2 of the SM and $D(T,P)$ and $N_c(T,P)$ shown in Figs. 3(b) and 3(c), respectively, all reported in the SM. By estimating the (T,P) state points where $\log_{10} J/(\mathrm{m}^{-3}\,\mathrm{s}^{-1}) = 15, 5, -5$ we have drawn the iso-J lines shown in Fig. 1.

barrier top and is related to the width of the critical region. The attachment rate f^+ can be approximated as $f^+ = 24 D N_c^{2/3}/\lambda^2$, where D is the diffusion coefficient of the supercooled water [shown in Fig. 3(b)] and $\lambda =$ 3.8 Å according to previous work [46]. Such an approximation successfully works at positive pressure [46]. We test it at negative pressure by computing f^+ rigorously as in Ref. [63] from $\langle [N(t) - N(0)]^2 \rangle = 2 f^+ t$, at $T = 240$ K for $P = -300, -1700, -2900$ bar finding good agreement, as reported in SM (the deviations do not affect the resulting value of J).

The P dependence of ΔG_c is shown in Fig. 3(d). Then, we estimate J via Eq. (2). In Fig. 4(b), the returning of J at negative P is revealed. The maxima of J are found at $P < 0$ for all the explored T and mark the (T,P) conditions where homogeneous nucleation occurs more easily as recently suggested by Marcolli [21]. In this particular case, $J \sim 10^{22}$ m^{-3} s^{-1} for ($T = 230$ K, $P \sim -1200$ bar), $J \sim 10^{18}$ m^{-3} s^{-1} for ($T = 240$ K, $P \sim -1350$ bar), and $J \sim 10^{-1}$ m^{-3} s^{-1} for ($T = 250$ K, $P \sim -1750$ bar). Accordingly, the estimated surviving time τ of a water droplet with volume $V_{\mathrm{ice}} \sim 5$ cm^3 characteristic of the inclusion experiments at negative P [13,18] is $\tau \equiv (J V_{\mathrm{ice}})^{-1} \sim 2 \times 10^{-17}$ s at $T = 230$ K, $\tau \sim 2 \times 10^{-13}$ s at $T = 240$ K, and $\tau \sim 2 \times 10^{6}$ s at $T = 250$ K. Thus, this work suggests that 245–250 K is the minimum T at which one can study macroscopic samples of water at $P < 0$ without freezing the entire sample in a few seconds.

Finally, we compute the isonucleation rate lines for TIP4P/Ice (representing the loci of points in the P-T plane where the nucleation rates have identical values). They are presented in Fig. 1 for $\log_{10} J/(\mathrm{m}^{-3}\,\mathrm{s}^{-1}) = 15, 5, -5$. As can be seen, the isonucleation rate lines present reentrant behavior. The curve $\log_{10} J/(\mathrm{m}^{-3}\,\mathrm{s}^{-1}) = 15$ is of particular interest as it can be regarded as an estimate of the experimental homogeneous nucleation line (HNL) [9] where freezing of droplets of a few microns occurs in a few seconds and cannot be avoided, thus, representing the solid-liquid limit of stability. In the 230 K isotherm, $\log_{10} J/(\mathrm{m}^{-3}\,\mathrm{s}^{-1}) = 15$ occurs at $P = 1$ bar (see also Fig. 1). The results of this work suggest that the HNL presents reentrant behavior, another anomaly of water arising at the confluence of low T and negative P [64,65] that, to the best of our knowledge, has not been reported before.

In conclusion, we use computer simulations of the TIP4P/Ice water model to estimate the size of the critical nucleus N_c along three isotherms $T = 230$ K, $T = 240$ K, and $T = 250$ K. We cover from typical positive coexistence pressures until approaching the liquid-gas kinetic stability curve (under 100 ns of observation). We show how N_c does not change monotonically exhibiting a minimum at negative P and increasing again in the vicinity of the stability limit. Accordingly, the nucleation rate J and the surface tension γ show a retracing behavior, with a maximum of J and a minimum of γ both occurring at negative P. Our findings reveal new water anomalies as the retracing behavior of N_c, γ, and J along the isotherms when going from positive to negative pressures. We also predict anomalous behavior of the homogeneous nucleation line, which again presents reentrant behavior at negative pressures. This can be regarded as a smoking gun of the reentrance of the melting curve which can be evaluated experimentally only up to moderate values of negative pressures [13,15–18].

The authors acknowledge Project No. PID2019–105898GB-C21 of the Ministerio de Educacion y Cultura. V. B. acknowledges the support from the European Commission through the Marie Skłodowska-

Curie Fellowship No. 748170 ProFrost. P. M. d. H. acknowledges the financial support from the Formacion Personal Investigador Grant No. BES-2017-080074. C. P. L thanks Ministerio de Educacion y Cultura for a predoctoral Formacion Profesorado Universitario Grant No. FPU18/03326 and also Ayuntamiento de Madrid for a Residencia de Estudiantes grant. The authors acknowledge the computer resources and technical assistance provided by the RES and the Vienna Scientific Cluster (VSC).

*vbianco283@gmail.com
†cvega@ucm.es

[1] A. Gettelman, X. Liu, S. J. Ghan, H. Morrison, S. Park, A. J. Conley, S. A. Klein, J. Boyle, D. L. Mitchell, and J.-L. F. Li, J. Geophys. Res. **115**, D18216 (2010).
[2] I. Coluzza *et al.*, Atmosphere-Ocean **8**, 138 (2017).
[3] J. Nitzbon, S. Westermann, M. Langer, L. C. P. Martin, J. Strauss, S. Laboor, and J. Boike, Nat. Commun. **11**, 2201 (2020).
[4] G. John Morris and E. Acton, Cryobiology **66**, 85 (2013).
[5] M. Bar Dolev, I. Braslavsky, and P. L. Davies, Annu. Rev. Biochem. **85**, 515 (2016).
[6] K. Broekaert, M. Heyndrickx, L. Herman, F. Devlieghere, and G. Vlaemynck, Food Microbiol. **28**, 1162 (2011).
[7] J. Russo, F. Romano, and H. Tanaka, Nat. Mater. **13**, 733 (2014).
[8] R. Bintanja, G. J. van Oldenborgh, S. S. Drijfhout, B. Wouters, and C. A. Katsman, Nat. Geosci. **6**, 376 (2013).
[9] J. R. Espinosa, A. Zaragoza, P. Rosales-Pelaez, C. Navarro, C. Valeriani, C. Vega, and E. Sanz, Phys. Rev. Lett. **117**, 135702 (2016).
[10] H. Niu, Y. I. Yang, and M. Parrinello, Phys. Rev. Lett. **122**, 245501 (2019).
[11] E. Sanz, C. Vega, J. R. Espinosa, R. Caballero-Bernal, J. L. F. Abascal, and C. Valeriani, J. Am. Chem. Soc. **135**, 15008 (2013).
[12] J. Green, D. Durden, G. Wolf, and C. Angell, Science **249**, 649 (1990).
[13] M. E. M. Azouzi, C. Ramboz, J.-F. Lenain, and F. Caupin, Nat. Phys. **9**, 38 (2013).
[14] P. Netz, F. Starr, H. Stanley, and M. Barbosa, J. Chem. Phys. **115**, 344 (2001).
[15] S. J. Henderson and R. J. Speedy, J. Phys. Chem. **91**, 3069 (1987).
[16] Q. Zheng, D. Durben, G. Wolf, and C. Angell, Science **254**, 829 (1991).
[17] A. R. Imre, H. J. Maris, and P. R. Williams, in *Liquids Under Negative Pressure: Proceedings of the NATO Advanced Research Workshop of Liquids Under Negative Pressure Budapest, Hungary* (Springer, Dordrecht, 2002), https://doi.org/10.1007/978-94-010-0498-5.
[18] F. Caupin, J. Non-Cryst. Solids **407**, 441 (2015).
[19] P. Gallo, K. Amann-Winkel, C. A. Angell, M. A. Anisimov, F. Caupin, C. Chakravarty, E. Lascaris, T. Loerting, A. Z. Panagiotopoulos, J. Russo, J. A. Sellberg, H. E. Stanley, H. Tanaka, C. Vega, L. Xu, and L. G. M. Pettersson, Chem. Rev. **116**, 7463 (2016).
[20] P. Montero de Hijes, E. Sanz, L. Joly, C. Valeriani, and F. Caupin, J. Chem. Phys. **149**, 094503 (2018).
[21] C. Marcolli, Sci. Rep. **7**, 16634 (2017).
[22] H. Kanno, R. J. Speedy, and C. A. Angell, Science **189**, 880 (1975).
[23] J. L. F. Abascal, E. Sanz, R. García Fernández, and C. Vega, J. Chem. Phys. **122**, 234511 (2005).
[24] P. G. Debenedetti, F. Sciortino, and H. Zerze, Science **369**, 289 (2020).
[25] B. Hess, C. Kutzner, D. van der Spoel, and E. Lindahl, J. Chem. Theory Comput. **4**, 435 (2008).
[26] T. Matsui, T. Yagasaki, M. Matsumoto, and H. Tanaka, J. Chem. Phys. **150**, 041102 (2019).
[27] A. Falenty, T. C. Hansen, and W. F. Kuhs, Nature (London) **516**, 231 (2014).
[28] See Supplemental Material at http://link.aps.org/supplemental/10.1103/PhysRevLett.126.015704 for a detailed description of the numerical methods and results (seeding, direct coexistence, mislabeling, thermodynamic integration and attachment rates) of this work and the fitting curves shown in the main text.
[29] M. Conde, C. Vega, G. Tribello, and B. Slater, J. Chem. Phys. **131**, 034510 (2009).
[30] R. J. Speedy, J. Phys. Chem. **86**, 982 (1982).
[31] L. Rovigatti, V. Bianco, J. Tavares, and F. Sciortino, J. Chem. Phys. **146**, 041103 (2017).
[32] P. G. Debenedetti, J. Phys. Condens. Matter **15**, R1669 (2003).
[33] P. W. Bridgman, Proc. Am. Acad. Arts Sci. **47**, 441 (1912).
[34] R. J. Speedy and C. A. Angell, J. Chem. Phys. **65**, 851 (1976).
[35] P. H. Poole, F. Sciortino, U. Essmann, and H. E. Stanley, Nature (London) **360**, 324 (1992).
[36] C. U. Kim, B. Barstow, M. W. Tate, and S. M. Gruner, Proc. Natl. Acad. Sci. U.S.A. **106**, 4596 (2009).
[37] K. Stokely, M. G. Mazza, H. E. Stanley, and G. Franzese, Proc. Natl. Acad. Sci. U.S.A. **107**, 1301 (2010).
[38] V. Bianco and G. Franzese, Sci. Rep. **4**, 4440 (2014).
[39] J. C. Palmer, F. Martelli, Y. Liu, R. Car, A. Z. Panagiotopoulos, and P. G. Debenedetti, Nature (London) **510**, 385 (2014).
[40] G. Pallares, M. El Mekki Azouzi, M. A. González, J. L. Aragones, J. F. Abascal, C. Valeriani, and F. Caupin, Proc. Natl. Acad. Sci. U.S.A. **111**, 7936 (2014).
[41] A. Nilsson and L. G. Pettersson, Nat. Commun. **6**, 8998 (2015).
[42] F. Perakis, K. Amann-Winkel, F. Lehmkühler, M. Sprung, D. Mariedahl, J. A. Sellberg, H. Pathak, A. Späh, F. Cavalca, D. Schlesinger, A. Ricci, A. Jain, B. Massani, F. Aubree, C. J. Benmore, T. Loerting, G. Grübel, L. G. M. Pettersson, and A. Nilsson, Proc. Natl. Acad. Sci. U.S.A. **114**, 8193 (2017).
[43] V. Bianco and G. Franzese, J. Mol. Liq. **285**, 727 (2019).
[44] P. Gallo, T. Loerting, and F. Sciortino, J. Chem. Phys. **151**, 210401 (2019).
[45] X.-M. Bai and M. Li, J. Chem. Phys. **122**, 224510 (2005).
[46] J. R. Espinosa, E. Sanz, C. Valeriani, and C. Vega, J. Chem. Phys. **141**, 18C529 (2014).
[47] J. R. Espinosa, C. Vega, C. Valeriani, and E. Sanz, J. Chem. Phys. **144**, 034501 (2016).

[48] J. R. Espinosa, C. Navarro, E. Sanz, C. Valeriani, and C. Vega, J. Chem. Phys. **145**, 211922 (2016).
[49] J. R. Espinosa, C. Vega, and E. Sanz, J. Phys. Chem. C **122**, 22892 (2018).
[50] Y. Lifanov, B. Vorselaars, and D. Quigley, J. Chem. Phys. **145**, 211912 (2016).
[51] F. Leoni, R. Shi, H. Tanaka, and J. Russo, J. Chem. Phys. **151**, 044505 (2019).
[52] P. Montero de Hijes, J. R. Espinosa, E. Sanz, and C. Vega, J. Chem. Phys. **151**, 144501 (2019).
[53] P. Montero de Hijes, J. R. Espinosa, V. Bianco, E. Sanz, and C. Vega, J. Phys. Chem. C **124**, 8795 (2020).
[54] P. Montero de Hijes, K. Shi, E. Noya, E. Santiso, K. Gubbins, E. Sanz, and C. Vega, J. Chem. Phys. **153**, 191102 (2020).
[55] A. O. Tipeev, E. D. Zanotto, and J. P. Rino, J. Phys. Chem. C **122**, 28884 (2018).
[56] B. C. Knott, V. Molinero, M. F. Doherty, and B. Peters, J. Am. Chem. Soc. **134**, 19544 (2012).
[57] R. G. Pereyra, I. Szleifer, and M. A. Carignano, J. Chem. Phys. **135**, 034508 (2011).
[58] T. Dasgupta, G. M. Coli, and M. Dijkstra, ACS Nano **14**, 3957 (2020).
[59] H. Niu, L. Bonati, P. M. Piaggi, and M. Parrinello, Nat. Commun. **11**, 2654 (2020).
[60] N. E. Zimmermann, B. Vorselaars, D. Quigley, and B. Peters, J. Am. Chem. Soc. **137**, 13352 (2015).
[61] W. Lechner and C. Dellago, J. Chem. Phys. **129**, 114707 (2008).
[62] R. Becker and W. Döring, Ann. Phys. (Berlin) **416**, 719 (1935).
[63] S. Auer and D. Frenkel, Nature (London) **409**, 1020 (2001).
[64] Y. E. Altabet, R. S. Singh, F. H. Stillinger, and P. G. Debenedetti, Langmuir **33**, 11771 (2017).
[65] V. Holten, C. Qiu, E. Guillerm, M. Wilke, J. Ricka, M. Frenz, and F. Caupin, J. Phys. Chem. Lett. **8**, 5519 (2017).